Nanoionics: ion transport and electrochemical storage in confined systems

The past two decades have shown that the exploration of properties on the nanoscale can lead to substantially new insights regarding fundamental issues, but also to novel technological perspectives. Simultaneously it became so fashionable to decorate activities with the prefix 'nano' that it has become devalued through overuse. Regardless of fashion and prejudice, this article shows that the crystallizing field of 'nanoionics' bears the conceptual and technological potential that justifies comparison with the well-acknowledged area of nanoelectronics. Demonstrating this potential implies both emphasizing the indispensability of electrochemical devices that rely on ion transport and complement the world of electronics, and working out the drastic impact of interfaces and size effects on mass transfer, transport and storage. The benefits for technology are expected to lie essentially in the field of room-temperature devices, and in particular in artificial self-sustaining structures to which both nanoelectronics and nanoionics might contribute synergistically.

J. MAIER

is in the Max-Planck-Institut für Festkörperforschung, 70569 Stuttgart, Germany.
e-mail: s.weiglein@fkf.mpg.de

The triumph of electronics in both science and daily life relies, on the one hand, on the availability of solid materials in which atomic constituents exhibit negligible mobilities whereas electronic carriers can be easily excited and transferred; and, on the other, on the necessity of fast and precise information exchange. However, electronic devices cannot satisfy all the technological needs of our society: as far as the transformation of chemical to electrical energy or the chemical storage of electrical energy is concerned — as is possible in batteries and fuel cells, or as far as the transformation of chemical in electrical information is concerned — as verified in (electro)chemical sensors, electrochemical devices are indispensable[1–4]. Solid electrochemical devices use the fact that (at least) one ionic component is immobile whereas another ionic component is highly mobile, and hence combine mechanical durability and electrochemical functionality. Such solids may be solid electrolytes — that is, pure ion-conducting solids — but they may also be mixed conducting solids that exhibit both significant electronic and ionic conductivities and can, for example, be used as powerful electrodes. Mixed conductors can also be used as key materials in related devices such as chemical sensors, chemical filters, chemical reactors and electrochromic windows. Figure 1 provides a schematic overview by using the example of oxide ion conductivity. Beyond that, the study of mixed conductors offers a general phenomenological approach to electrically relevant solids in which the pure ionic and the pure electronic conductor appear as special cases.

In the nanometre regime, interfaces are so closely spaced that their influence on the overall property can become significant if not prevailing. It can even no longer be taken for granted that one can assume semi-infinite boundary conditions; in other words, it cannot be taken for granted that, with increasing distance, the impact of the interface dies off to the bulk value, because the next interface might already be perceptible. In interfacially controlled materials the overall impact of the interfacial regions increases with decreasing size. As long as their local influence is identical to or comparable with that of isolated interfaces we may use the term 'trivial size effects', whereas the term 'true size effects' implies that interfaces perceive each other[5–8]. As long as we can ignore the effect of curvature this distinction is possible.

Nanoelectronics[9–12] is essentially based on the quantum-mechanical confinement effect, a true size effect as a consequence of which the energy of delocalized electrons increases with decreasing size. As far as electronic devices[13] are concerned, trivial size effects are important in varistors (insulating grain boundaries become conductive under bias), PCT ceramics (resistance shows a

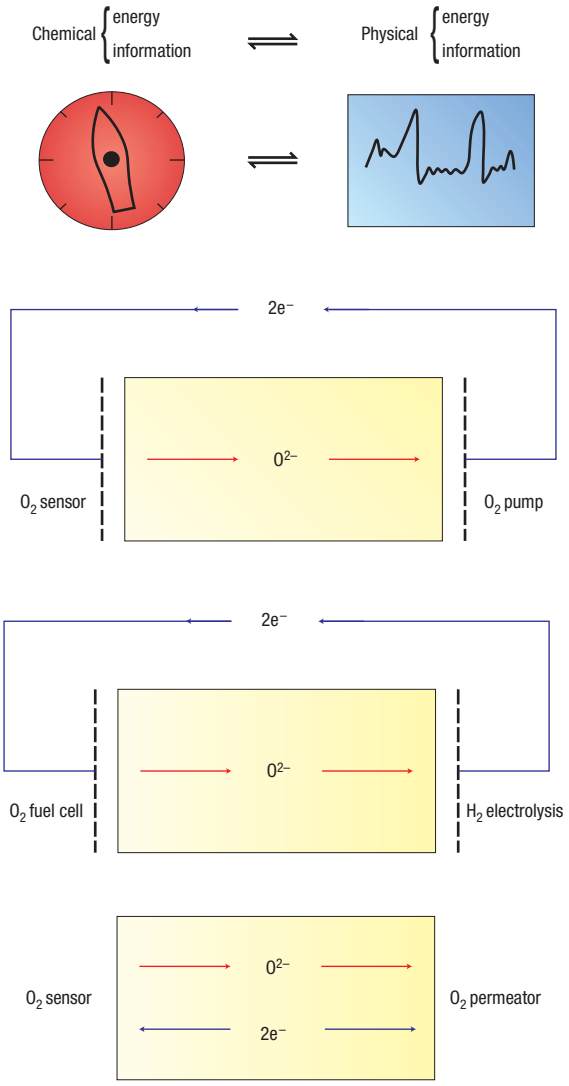

Figure 1 Electrochemical devices relying on ionic and mixed electronically and ionically conducting solids enable the transformation of chemical energy or information into electrical energy or information (or vice versa). Top cell: by using O^{2-}-conducting electrolytes, oxygen can be pumped from one side to the other by applying an electrical field. Under open-circuit conditions, different partial pressures of oxygen give rise to a cell voltage that can be used as a sensor signal. Middle cell: high voltages and high power output without being limited by Carnot efficiency can be achieved in a fuel-cell arrangement in which the chemical formation energy of water is directly converted into electrical energy. The reversal of the process is relevant for hydrogen generation at elevated temperatures. Bottom cell: in mixed conductors, oxygen is dissolved in the solid and can permeate through. This can be used to purify gases, to increase the effective electrode area in fuel cells or to store oxygen. The storage aspect is relevant for equilibrium gas sensors (for example oxygen detection through conductivity changes of mixed conductors), or — in particular if H^+ and Li^+ are used instead of O^{2-} — for energy technology (storage of H_2 or Li); the compositional variation can also be exploited with respect to other properties (for example optical properties in electrochromic windows, or mechanical properties).
Reprinted with permission from ref. 91; http://www.tandf.co.uk.

positive temperature coefficient[14]) or Taguchi sensors (adsorbed gases alter the charge-carrier concentration on the surface of semiconductors[15]), in which the interaction between interfacial chemistry and electrical resistance is decisive. Note that in these examples solid-state ionics has a major role.

It has been shown during the past two decades that ionic transport properties are also drastically changed at interfaces, leading to significant trivial and true size effects that at a sufficient number density of interfaces can become prevalent for the whole material[8,16–20]. Not only can an insulator or an electronic conductor be turned into an ionic conductor or an anion conductor into a cation conductor, but artificial conductors can also be generated that are unavailable otherwise. Given this enormous influence of interfaces on ion transport, and given the indispensability of electrochemical devices, it can be expected — and this will be set out in more detail below — that the importance of nanoionics[5–8,16–21] to electrochemistry will be similar to that of nanoelectronics to semiconductor physics. One necessary condition is that the nanostructured arrangement be sufficiently stable. Even though this point is naturally more critical than in nanoelectronics, it has been shown in many cases that metastable interfaces can be durable even up to quite high temperatures.

SIZE EFFECTS IN SOLID-STATE IONICS

Let us first consider the implementation of an interface in a solid system and study its impact on the ionic transport properties. In general this process breaks symmetry by introducing a structural discontinuity. In contrast with the bulk, where electroneutrality must be obeyed, at the interface a narrow charged zone, the so-called space-charge zone, is tolerable and even thermodynamically necessary[13,22–26]. The effects on both electrons and ions can be quantitatively studied, if an abrupt structural change (see Fig. 2) at the interface is assumed[25,26]. Here, the reader may be more interested in a qualitative approach and for this purpose it is advisable to consider the different charge carriers — being strongly coupled by the condition of electroneutrality in the bulk — as independent. Of course, the deviation from charge neutrality results in an electrical field that limits the magnitude and spatial extent of the carrier redistribution. Before considering the impact on charge-carrier concentration more specifically, let us note that because of the different structure of the interfacial core, mobilities change there too. Whether such core effects or space-charge effects are more important for the transport depends on the parameters of the materials and the current direction. If we consider, for example, transport along interfaces, space-charge transport is typically significant if bulk mobilities are high, bulk concentrations are small and carriers are accumulated, whereas in low-mobility materials grain boundaries are likely to offer enhanced mobilities.

Now let us concentrate on the thermodynamically required space-charge effects and consider the simplest case, namely grain boundaries in chemically homogeneous materials. As a result of the difference in structure between boundary and bulk, they are loci of charge separation: in polycrystalline AgCl (Fig. 2d) and polycrystalline CaF_2 the space-charge zone adjacent to the grain boundaries exhibits enhanced vacancy conductivity

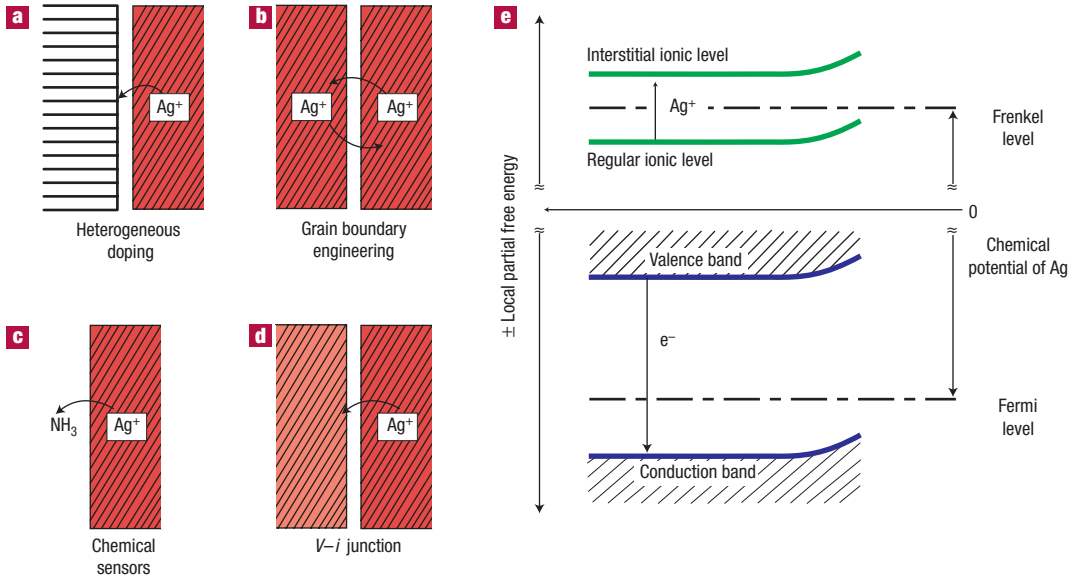

Figure 2 Ion redistribution at equilibrium. **a–d**, Four prototype situations involving boundaries to solid ion conductors (using Ag^+ conductor as an example). **a**, Contact to an insulating phase that adsorbs Ag^+; **b**, grain boundary; **c**, contact to an acid–base active gas phase; **d**, contact to a second Ag^+ conductor. **e**, The ionic excitations (Ag^+ transfer from a regular site to an interstitial site, leaving behind a vacancy) can be represented in a (partial free) energy-level diagram, as is commonly used for electronic excitations. At boundaries the charging leads to bending of the levels. The coupling of the ionic (Ag^+, top) and electronic (bottom) pictures is determined by the (Ag) stoichiometry. A given interfacial charge leads to predictable consequences with respect to ionic and electronic carrier concentrations. Reprinted from ref. 92 with kind permission of Springer Science and Business Media.

(silver ion vacancies and fluoride ion vacancies[17]). In nanocrystalline samples especially, this interfacial effect is dominant in overall transport[27]. It can be chemically enforced and enhanced by contamination with NH_3 and SbF_5 (ref. 17), respectively. In $SrTiO_3$ or CeO_2 the grain boundaries show a positive excess charge, which leads to a depression of hole and oxygen vacancy concentrations there and hence to a decrease in ionic and electronic (in the p-regime) conductivities (Fig. 3, top middle)[28–34]. As both carriers are needed for (chemical) oxygen diffusion, the simultaneous depression of both types of conductivity results in a significant chemical resistance exerted by the boundary and observed during an experiment *in situ* in which the oxygen stoichiometry is varied and locally recorded[33]. Whereas the positively charged holes are depleted at such boundaries, the negatively charged conduction electrons have to be accumulated. This phenomenon is clearly seen in (weakly Gd-doped) CeO_2, in which the grain boundaries become n-type conducting whereas the bulk is ionically conducting[28,29,34].

It turned out that a very efficient method of directing or enhancing the space-charge effect is to decorate the grain boundaries with surface-active second-phase particles. Let us specifically consider the addition of fine-grained insulating Al_2O_3 particles to AgCl in which the defect concentration is quite small but in which the defects possess a significant mobility. Then we refer to the situation displayed in Figs 2a and 4d. As the basic oxide acts to adsorb the mobile cation, excess cation vacancies are necessarily formed in the AgCl matrix adjacent to the contact. By this heterogeneous doping process[35] insulators can be transformed into conductors (for example $LiI:Al_2O_3$ (refs 36, 37), which was in fact the first composite electrolyte to be studied), anion conductors into cation conductors (for example $TlCl:Al_2O_3$ (ref. 38)), interstitial conductors into vacancy conductors ($AgCl:Al_2O_3$ (ref. 35)), or even superionic transitions can be provoked ($AgI:Al_2O_3$ (ref. 39)). By using mesoporous insulator phases with pore sizes of a few nanometres, this effect can be driven towards very high conductivities[40,41]. Similarly, SiO_2 is active in adsorbing anions; in this way the F^- conductivity in fluorides can be distinctly enhanced[42]. It has recently been shown that heterogeneous doping can even be used to significantly increase the Li^+ conductivity of liquid non-aqueous Li^+ electrolytes[43] (an effect that will be revisited below). The mechanism is the same — in both cases anions are adsorbed; in CaF_2, F^- is removed from the strongly bonded ion arrangement leaving the uncompensated cation (and hence an anion vacancy), whereas in the liquid the Li^+ ions, which are significantly associated with the anions in the bulk, are set free as a consequence of anion adsorption in the contact zones.

A beneficial effect of oxide particles on polymeric Li^+ electrolytes has also been reported[44,45]. As a large fraction of the Li salt is also expected to be undissociated, contributions by a similar mechanism are likely (see also ref. 46).

The inverse effect of a liquid phase on a solid conductor is also known; even gas phases (Fig. 2c) can be used if they are acid–base active, for example NH_3 in the case of AgCl (ref. 47) or BF_3 in the case of CaF_2 (ref. 17), leading to a novel sensor principle.

At the contact of two ionic (mixed) conductors (in addition to a possible charging of the proper interfacial core) a redistribution over both space-charge layers is thermodynamically required[48] (Fig. 2d). This explains the huge conductivity enhancement effects observed in two-phase systems of two silver halides[48,49] or in the CaF_2/BaF_2 heterolayer systems[50,51] (Fig. 3, top left).

The modifications affect not only transport; storage anomalies, too, occur at interfaces[17,20,52,53]. Even if the abrupt structural model is valid and the chemical potential of the element to be stored is spatially invariant within a given phase, a striking effect can occur at the contact[20]. Consider a compound MX that can be stored in neither phase

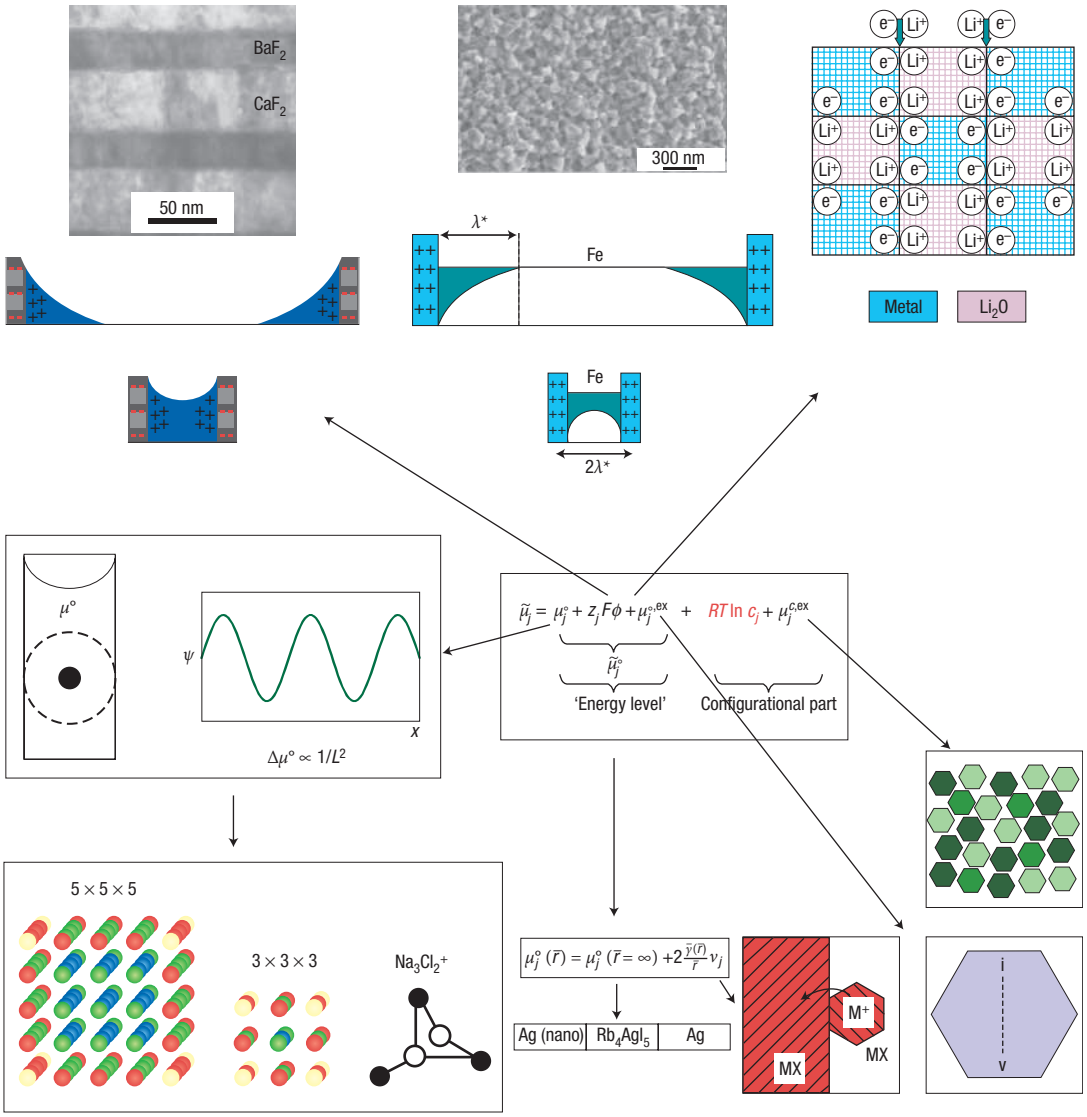

Figure 3 Size effects classified according to their contribution to the total chemical potential $\tilde{\mu}$ (see the text). Top, from left to right: penetrating accumulation zones in CaF_2/BaF_2 heterolayers, penetrating depletion zones in $SrTiO_3$ nanoceramics, and heterogeneous storage of Li in Li_2O/Ru nanocomposites as examples of electrostatic effects. Middle left: variation of the free formation energy of a localized defect or delocalized electron if confinement becomes perceptible. Bottom left: impact of edges and corners on the surface energy, breakdown of crystal structure. Bottom middle: effects of curvature on the activity of components and the distribution of ions. Bottom right: effects on interaction (interstitials (i) and vacancies (v) cannot separate) and configurational effects (see the text for more details).

A nor phase B; let us assume that in phase A storage is impossible because X^- cannot be accepted (but M^+ can), whereas in phase B the solution of M^+ cations is forbidden (but not that of X^-). Job sharing, however, would allow the composite to store up to (typically) a monolayer of MX at the heterojunction. This storage effect will be considered again in the context of Li batteries (in which $X^- = e^-$; see Fig. 3, top right).

As already mentioned, at interfaces mobilities are altered as well; furthermore, significantly changed local reactivities are expected and have been observed in several investigations (see, for example, ref. 54). A substantial finding in the present context is that point defects act as most efficient acid–base active centres on the surface, as demonstrated by homogeneous and heterogeneous doping of heterogeneous catalysts[55,56].

These examples should convince the reader not only of the richness of the field but also of the powerful additional degree of freedom when leaving single crystals and using interfacially controlled materials.

Now let us briefly consider the thermodynamic consequences of the introduction of point defects (Fig. 3, middle; ref. 16). The generation of a single defect is connected with a severe expenditure of energy that is not ironed out by the alteration of the local (vibrational) entropy; the formation of defects therefore costs locally free energy (see the $\mu°$ term in Fig. 3) and would forbid their existence in thermodynamic equilibrium were there not the significant free-energy gain caused by the huge number of microscopically different but energetically equivalent possibilities of distributing these defects (gain in configurational entropy). The different aspects are expressed in Fig. 3 in terms of various contributions to the chemical potential of a defect. Note that the chemical potential of a species measures the increase in the total free energy if the concentration (c) of this species is marginally increased; it is therefore the relevant measure when the concentration that corresponds to the minimum of the free energy is to be discovered. If defects are dilute and randomly distributed, the well-known

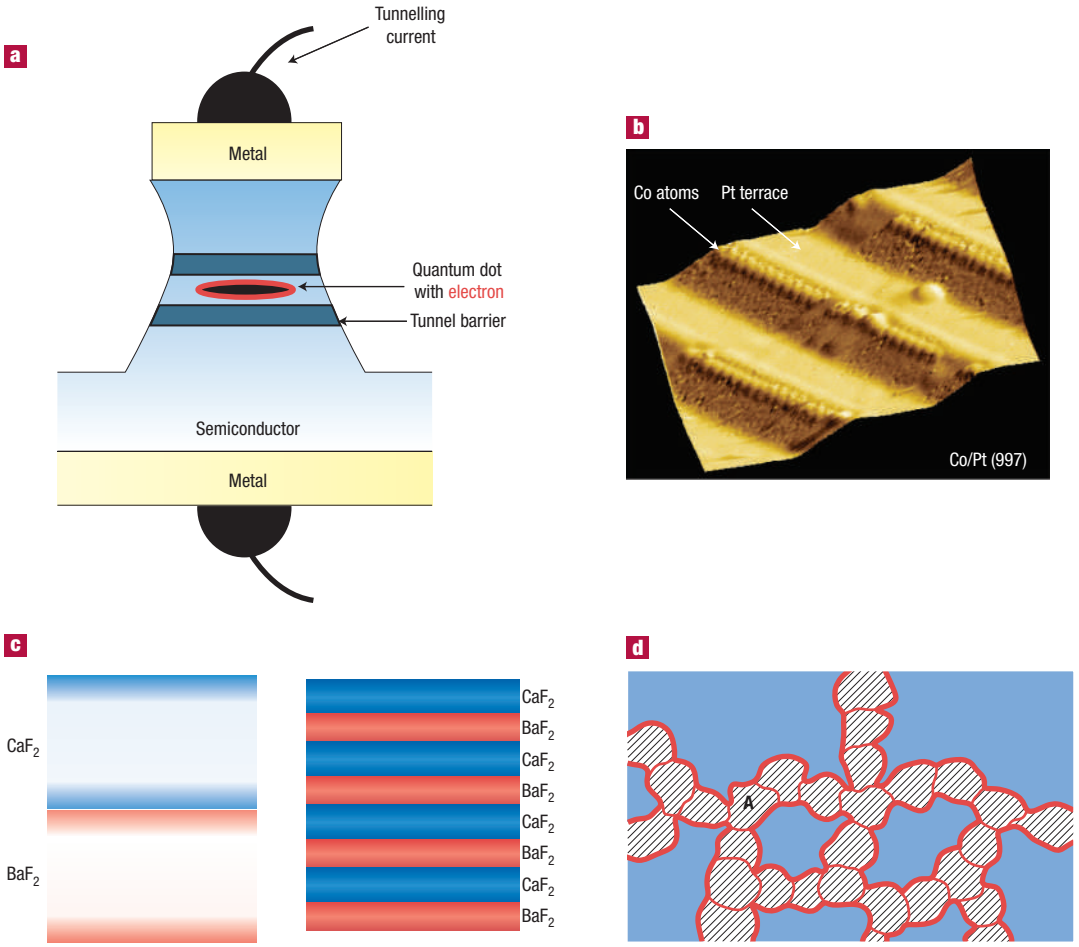

Figure 4 Different dimensionalities of interfacially controlled systems in solid-state electronics and ionics. **a**, Quantum dots in nanoelectronics[11]. **b**, Nanowires as nanomagnets. **c**, Nano-sized ionic heterolayers as artificial ion conductors. **d**, nanocomposite ion conductors consisting of insulator A in ion-conducting matrix MX. Part **a** reprinted from ref. 6. Copyright (2002), with permission from Elsevier. Parts **b** and **c** reprinted from refs 93 and 50, respectively, with permission from *Nature*.

Boltzmann form results ($\mu = \mu^\circ + RT\ln c$). Corrections to this occur at higher concentrations where the defects feel each other and/or feel the limited number of available sites (or quantum states). This leads to corrections in terms of energy and entropy (μ^{ex}). (Another correction becomes necessary if concentration gradients are so steep in the interfacial regions that the local properties depend on them and not only on the local value.) In the bulk we meet as many positive as negative charge carriers. This is different at interfaces, with the consequence that electrical field terms ($zF\phi$, where z is charge number, F is Faraday's constant and ϕ is electrical potential) have to be considered explicitly. The total chemical potential, which also contains the electrical effects, is usually called electrochemical potential (and termed $\tilde{\mu}$ in Fig. 3). If the structure does not change abruptly at an interface, the local formation term is a function of the distance. This is particularly important if the interfacial contact results in severe strain, as frequently occurs in epitaxial thin films. The peculiarities of the interfacial situation can even lead to interfacial phase transformations[57,58]. Finally, we also have to take account of the three-dimensional shape of the grains, which is reflected by its (mean) curvature ($1/\bar{r}$, where $\bar{r}$ is mean radius). An increased curvature leads to an enhanced internal pressure that augments the chemical potential by (at least) $2(\bar{\gamma}/\bar{r})v$, where v is the partial molar volume.

It is important in our context that all these contributions (and the list given is not exhaustive) give rise to, or are relevant in terms of, true size effects, the most important of which are addressed in Fig. 3 (for more details see refs 7, 16). Let us consider some of them, and first ignore curvature; that is, let us concentrate on thin films ($1/\bar{r} = 0$). If the spacing of the interfaces is perceptibly less than the effective width of space-charge layers, these layers overlap and the sample is charged throughout. Such effects with regard to accumulation layers (Fig. 3, top left) are discussed in epitaxially grown ionic heterolayers[59] whose thickness has been varied from 1 nm to 1 μm or in AgI nanoplates[60] in which heterolayers appear inherently, which represent the best binary solid electrolyte material at room temperature known so far. The counterpart — namely, penetrating depletion layers (Fig. 3, top middle) — has recently been observed in nanocrystalline $SrTiO_3$ (ref. 61). In the latter case the effective space-charge width is much larger than for the accumulation layers because the screening is much less and as the dielectric constant in $SrTiO_3$ is quite high. The top right panel in Fig. 3 shows the size effect on the storage capacity already mentioned.

In practice, although not a bad approximation in many situations[37,62], the structural change at the interface will not be restricted to one or two atomic layers; in some cases elastic effects can penetrate

quite deeply and — if the interfacial spacing is very small — even penetrate the whole sample. Then the μ° term (Fig. 3) will be dependent on position and will be different from the value of the bulk in a large single crystal. However, even if the perfect structure decays in a step-function way, very narrowly spaced interfaces can change the formation energy and entropy of a defect. Let us first consider the energetic part in terms of two phenomena. First, the introduced defect polarizes the neighbourhood and the effective sphere of influence ranges much more widely than the atomic size (Fig. 3, middle left). If this sphere of influence is comparable to or larger than the spacing, this confinement will severely alter the energies[7,16]. This is the classical counterpart of the confinement effect that delocalized electrons experience; they can be much more extended and can perceive the boundaries much earlier. As electrons and ions perceive confinement with different sensitivities, the exploration of size effects of mixed conductors is of fundamental importance. Second, in the same way that electrons and holes cannot separate in tiny crystals[9], this is true for ionic defect pairs or pairs of ionic and electronic defects (Fig. 3, bottom right).

In addition, entropic contributions are affected by the particle size. First, the vibrational properties differ and hence the vibrational entropy. Second, in tiny systems the small number of atoms does not allow one to draw the usual statistical conclusions about the configurational entropy. At best an ensemble of nano-sized particles can be treated as a statistically significant ensemble (Fig. 3, bottom right). The consequence is that the conductivity (or reactivity) may vary significantly from particle to particle and may lead to peculiar effects.

In substantially curved crystals — that is, small ones — a size variation leads to variation in interfacial area, curvature and bulk volume. Like soap bubbles they experience an increased internal pressure (Fig. 3, bottom middle) and hence a greater chemical potential than that in a large single crystal. The most prominent consequence of this is the substantial decrease in the melting point of nanocrystals[63]. The (free) energetic difference shows up directly in the cell voltage of 'symmetrical' electrochemical cells that differ only in the grain size of active electrode components (for example in the all-solid-state cell in Fig. 3, bottom middle, which relates to the measurement of the excess free energy of nanocrystalline silver)[64,65]. For the same reason charging is also predicted if two particles of the same composition and orientation but different sizes come into contact[7]. It has already been mentioned that this excess contribution is proportional to the effective interfacial tension and inversely proportional to the effective radius as long as the surface tension stays constant. At tiny sizes the interfacial tension itself becomes a function of size, for a variety of reasons (such as the importance of edges and corners or the confinement of atoms within interfaces or edges; see Fig. 3, bottom left). At sizes of typically a few nanometres the macroscopic structure finally breaks down (Fig. 3, bottom left). In NaCl, for example, the rock salt structure is well established if the size is of the order of a few lattice constants; however, below that size completely different structures are thermodynamically stable[66]. Then we leave the regime of solid-state chemistry and enter the regime of cluster chemistry; accordingly, we leave the range of validity of our top-down approach, and a bottom-up approach becomes advisable.

MATERIALS STRATEGIES

So far it has become clear that the deliberate introduction of interfaces ('heterogeneous doping'[25]) is a powerful method of modifying the electrochemical properties of materials (see above; ceramics, polymers and liquids, but also glasses[67]) besides the conventional tools (i) of searching for novel ground structures and compositions, (ii) of varying temperature and stoichiometry, or (iii) of introducing impurities. The similarity of 'heterogeneous doping' to conventional, homogeneous doping (dissolution of foreign atoms) is striking because in both cases defects (but of different dimensionality) are irreversibly introduced, resulting in significant and quantifiable effects on charge-carrier density[68].

The benefit of narrowly spaced interfaces that act as fast pathways for ions or components lies not only in the enhanced effective conductivity but also in the possibility of rapid bulk storage resulting from the reduction of the effective diffusion length. Because the equilibration time is proportional to the square of the diffusion length, storage in nanosystems can be enormously fast. A size reduction from 1 mm to 10 nm reduces the equilibration time by 10 orders of magnitude. However, the same effect simultaneously sets a limit on the kinetic stability.

For 10 nm grains not to grow (on a timescale of years), the diffusion coefficient must be smaller than 10^{-20} cm^2 s^{-1}. This constraint does not contradict the material's electrochemical functionality because the diffusion coefficient, which is decisive for morphological stability, relates to the most sluggish component. (Typical values of diffusion coefficients in metals are between 10^{-30} and 10^{-20} cm^2 s^{-1}.) In addition, the danger of growth can be effectively diminished by the presence of second phases: Examples are the hetero-layers already touched upon (see Fig. 4c) or the nanocomposites in the context of Li-battery electrodes (see Fig. 5 and ref. 69).

For atomic-scale structures to exhibit sufficient stability, one has to engineer systems that are in spatial equilibrium (illustrative examples are the β-alumina ion conductors[70] (Fig. 6a), the high-temperature superconductors[71] or the alkali suboxides[72] in which conducting and non-conducting regions coexist on the atomic scale) or to rely on extremely low transport or reaction coefficients (as typically observed in covalent organic systems such as biopolymers).

To benefit from nanomaterials one can make use of confinement in one, two or three dimensions (Fig. 4). The last situation is met in nanodot systems, as represented by isolated grains or grain arrangements as in nanocrystalline ceramics. (Fig. 4a relates to nanoelectronics and displays a quantum dot.) Confinement in two dimensions is met in nanowires, nanotubes or nanoneedles. (The example

in Fig. 4b relates to one-dimensional magnets.) Thin films finally offer the possibility of a one-dimensional confinement. In all cases we may refer to single-phase or multiphase systems, such as are realized in nanocomposites (or core–shell structures and nanoporous systems) or nano-sized heterolayer films. Figure 4c, d gives examples relating to nanoionics.

The significance of the possibility of generating systems that rely on the integration of metastable subsystems in the nanometre range can hardly be overestimated. In this regime the distances involved are small enough to permit high storage and rapid exchange of energy and information on an accessible timescale, but the distances are not yet so small that kinetic stability with respect to transport and reaction has to be given up (Fig. 6); it is not accidental that the integration of biological functions (Fig. 6d) is essentially connected with nanostructuring. (Note that, in addition, biomolecules themselves are pronouncedly (meta)stable as a result of the strong covalent bonds.) It is generally expected that on this scale the introduction of higher dimensional defects or the integration or combination of subsystems can lead to non-equilibrium systems with a much higher information content than is possible at equilibrium ('soft materials science'[73]). Artificial nanomaterials of interest may be fabricated by artificial design, as in heterolayers, or be self-assembled, as in dissipative biological structures.

APPLICATIONS

It was stated above that nanosystems reveal their advantages typically at temperatures that are low or moderate. It is no coincidence that the most striking results in the field of electrochemical devices have been obtained in the context of Li batteries that work at room temperature.

In high-performance (secondary) Li batteries a reversible discharge–charge procedure has to be connected with high power density and capacity. The established way to achieve the first is to choose electrodes that accommodate Li without structural change; that is, to use intercalation compounds or — to put it more generally — to work within the homogeneity range of the Li-containing material. It is clear that this restricts the storage capacity severely. So it was a great step forward when Poizot *et al.*[74] recognized that CoO can almost reversibly take up Li down as far as reduction to the metal or even to the alloy. Although one is dealing with multiphase mixtures, the tiny transport lengths involved make the nanocomposite behave as a semi-fluid phase. The same effect could be verified for a variety of oxides, fluorides and nitrides[75,76]. In RuO_2, four Li per RuO_2 can be reversibly stored with an initial degree of conversion of virtually 100% (Fig. 5)[77].

Another striking phenomenon related to storage can be predicted to occur in such nanocomposites (Fig. 3, top right), which is of fundamental importance and has already been addressed briefly[6]. Let us consider the Li_2O/Ru composites that form *in situ* during the process of discharging a RuO_2-based Li battery. A significant uptake of Li does not seem possible because neither Ru nor Li_2O can store Li,

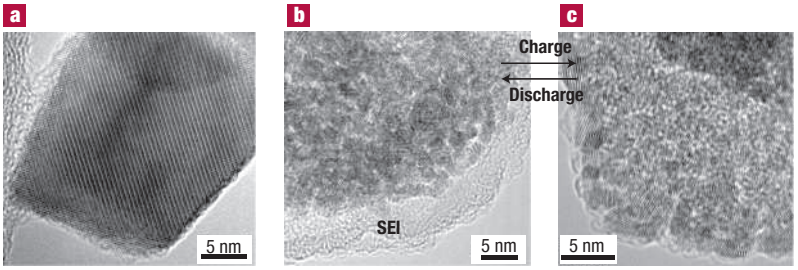

Figure 5 Reversibility of the redox reaction Li_2O + Ru $\leftrightarrow$ Li + RuO_2 in the nanocomposite upon Li extraction and incorporation[77]. **a**, Original situation; **b**, lithiated nanocomposite; **c**, delithiated nanocomposite. (SEI: interphase between electrode and electrolyte.)
Reprinted with permission from ref. 77.

the first because Li^+ cannot enter the structure (but e^- can) and in the second the electron is difficult to accommodate (but Li^+ can be). However, the synergistic situation discussed above and shown in Fig. 3 should apply, leading to the possibility of an extra storage of up to about a monolayer of Li^+ per boundary. In nanosystems in which the proportion of interfaces amounts to several tens of per cent by volume, this excess storage is able to deliver an explanation of pseudo-capacitive behaviour observed in many discharge curves close to 0 V with respect to Li. If the grains are so small that the space-charges overlap in Li_2O, this mechanism forms the bridge between a supercapacitor and a battery electrode and may offer a reasonable compromise between speed of discharge and capacity.

The small particle size is also able to explain other apparent anomalies in the discharge curve such as altered absolute voltage values, sloped discharge curves where flat curves would be expected for macro-sized samples, and the occurrence of inhomogeneous distribution of Li within the nanocrystalline electrode[20].

Nano-size effects are also important as far as the electrolyte is concerned. Composites in which LiI is infiltrated in nanoporous Al_2O_3 achieve conductivities as high as 10^{-3} S cm^{-1} at 60 °C, which makes them interesting candidates for battery electrolytes[41]. Oxide additions also proved beneficial in polymer electrolytes[44,45], which because of their high Li^+ conductivities and favourable mechanical properties, are candidates for solid electrolytes in high-performance Li batteries. In these polymer electrolytes, which solvate Li salts, intrinsic structural features extend from the atomistic (functional groups) to the nanometre (side chains, backbone) or even the micrometre (composite of crystalline and amorphous regions) range. In (non-aqueous) liquid electrolytes an important nano-sized heterogeneity is the metastable interface between the Li-rich electrodes and the liquid electrolytes[78], because its kinetic stability is the key criterion for the durability of the cell. Nano-sized heterogeneities can also be generated within the liquid. It has been recently shown (and already mentioned above) that admixtures of tiny SiO_2 particles to non-aqueous liquid electrolytes can substantially improve the battery electrolytes ('soggy sand')[79]. In this way this new class of electrolytes combines high conductivities with the favourable mechanical properties of soft matter (Fig. 6c). Cells using such electrolytes may be operated without a polymer spacer and offer greater safety. The higher

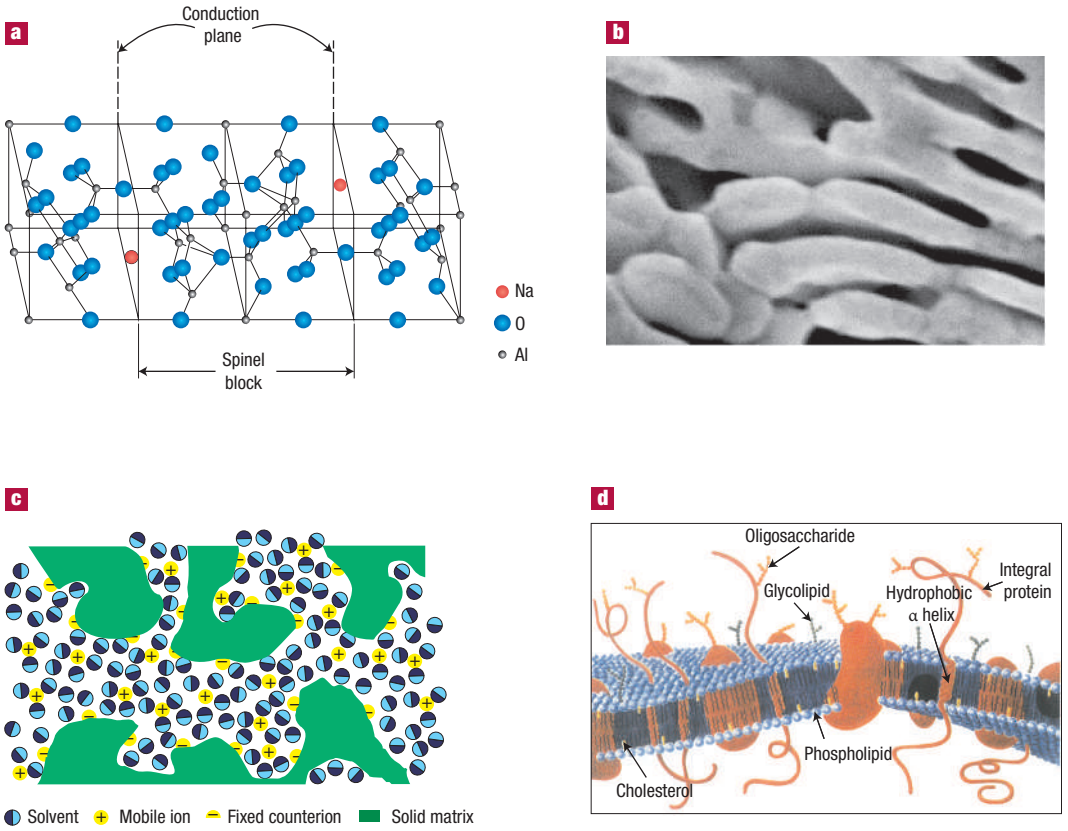

Figure 6 Integration of subfunctions in functional solids. **a**, Equilibrium structure of the ion conductor Na-β-alumina comprising conduction planes and insulating zones on an atomic level[70]. **b**, **c**, Solid–liquid nanocomposites with non-equilibrium morphology composed of an insulating and a conducting phase and combining mechanical strength and conductivity: **b**, Additive effects in AgCl(s)–$AgNO_3$(aq) composites[98]. **c**, Synergistic effects in 'soggy sand' (in which the solvent is a non-aqueous solvent, the anion is adsorbed counterion and the matrix is SiO_2 (ref. 43)) or Nafion (in which the solvent is water, the anion is covalently bonded sulphonic acid, and the matrix is an insulating organic backbone[94,95]). **d**, Lipid bilayer (containing membrane proteins) as the basic element of the plasma membrane of eukaryotic cells regulating the influx and efflux of matter[96]. Parts **a**–**c** reprinted from refs 97–99, respectively. Copyright (1992, 2002, 2000) with permission from Elsevier. Part **d** reprinted from ref. 96. Copyright (1995) with permission from John Wiley & Sons.

conductivity occurs when percolation between the boundary zones takes place: the particles either touch or are so close that the space–charge zones overlap severely.

In the end, the situation in the 'soggy-sand electrolytes' is quite similar to that of the Nafion electrolytes (used in low-temperature polymer-based fuel cells) except that, in the latter case, the negatively charged counterions are covalently built into the covalent network right from the beginning (Fig. 6c). The protons of these sulphonic acid groups are dissociated away in the tiny water channels interpenetrating the polymer matrix. Clearly, in Nafion the width of these channels is so small that finite size effects might be realized. Variants of this proton electrolyte address modifications of the framework, of the terminal groups as well as of the solvent, for example, using a polysiloxane network instead of the organic backbone, phosphoric acid groups instead of sulphonic acid groups or heterocycles instead of water. The ultimate goals are to prepare fully polymeric solvent-free networks providing high conductivities and to prevent the permeation of molecules such as water or methanol[80,81].

A different issue in the polymer-based fuel cells relates to the electrocatalysts. Here, too, the size is important. It has been shown[54] that metallic nanoparticles can provide a different catalytic activity, and size variation may be a possible way of ending up with a better electrode performance. Generally, enhanced reactivities may be caused by variations in defect concentration, by different fractions of atoms sitting in corners, edges or at the very surface and also by locally varied structure, composition and bonding.

In this context we should also note the attempts to use nanostructured matter for fast hydrogen storage[82–84].

Fuel cells operating at high temperatures have the advantage of improved electrode kinetics such that also hydrocarbons can be electrochemically converted without reforming. As far as the electrolyte is concerned, at these high temperatures the typically stronger activated bulk effects will dominate transport unless extremely tiny particles are used, whose morphology should be difficult to control. Nonetheless nanostructuring might be helpful, for example by trying to block electron conductivity in CeO_2. In particular, as regards the electrode a higher rate is feasible simply as a result of an enhanced interfacial area. In addition, however, size effects may be relevant for the electrode reaction itself in terms of modified reactivities. This is particularly relevant if the operation temperature of the fuel cells is to be lowered.

Similar aspects are valid for electrochemical (gas) sensors. Devices relying on complete equilibrium with the gas phase are sensors in which the gas is absorbed: the stoichiometry changes and so does the conductivity (see Fig. 1, bottom cell). The sensor sample itself has to be a mixed conductor. If bulk transport is rate-determining, nanostructuring can be helpful in reducing the transport length, whereas in interfacial control, nanostructuring can be helpful in directly influencing the mechanism. Because in this

sensor mode bulk diffusion is decisive for low cross-sensitivity, miniaturization may lead to a selectivity loss, albeit with a gain in response time.

Another important sensor type uses a purely ionically conducting material, namely a solid electrolyte (see Fig. 1, top cell) for which only equilibrium with the ions is achieved and the open-circuit potential is measured. Evidently, in this case the benefits of size effects with respect to the electrode reaction are more important than a potential improvement of the electrolyte conductivity. (The latter is more significant in the amperometric mode.)

Low-temperature (gas) sensors typically relate to the Taguchi principle in which neither is the gas incorporated nor equilibrium with the ions achieved in contact with typically semiconducting oxides. For oxygen, electrons are trapped by the adsorbed gas molecules, an effect that is reflected by the modified surface resistance[15]. Because it is the surface reaction that determines the signal response, nano-size effects are expected to be of significance for the response time. The same is true for drift effects. Although bulk diffusion is usually considered to be sluggish, a recent analysis for SnO_2 has shown that it is a sluggish subsequent step in the surface kinetics that prevents bulk equilibration in nanocrystals[85]. At any rate, nano-size effects are expected to influence performance. An enhanced sensor action with nanocrystalline oxide has indeed been reported for SnO_2 (refs 86, 87). The Taguchi principle can also be generalized to acid–base-active gases; electronic conductors then have to be replaced by ion conductors[88]. For NH_3 sensing, downsizing of the electrode contacts has already been shown to improve the sensor action significantly because of the greater sensitivity to surface properties[89].

Similar remarks apply to devices such as permeators, electrochromic windows, chemical storage devices (see Fig. 1) and photogalvanic cells[90], in which analogous principles are operative. At the end of this article, and as a pertinent outlook, stands the aspect of cellular integration of both electrochemical and electronic 'organs' on the nanometre scale. The integration of tiny sensor, actuator and computer elements — that is, of nano-sized 'hands' and 'legs' in addition to the computer 'brain', the whole ensemble being sustained by an energy-providing 'metabolism' — is expected to characterize future autonomous systems (similar to that sketched in Fig. 7) that could act as adaptive nanomachines. In this context, knowledge from biology (note that biological systems integrate fuel cell, sensor and actuator functions) and nanoscience would converge on learning from living systems how to combine artificial intelligence with artificial sensing and actuating organs into energetically autarchic systems.

Because the implementation of a high density of interfaces can lead to a substantial impact on the overall or even local ionic transport properties of solids and as nanostructured matter can be pronouncedly morphologically stable, the crystallizing field of nanoionics is expected to have a substantial role in future materials research. The span of relevant materials and preparation procedures is enormous, ranging from quasi one-dimensional heterolayers to three-dimensional composites on the one hand, and from tailored deposition procedures to self-organization on the other. Not only should new artificial materials come to the fore, but so should systems integrating ionic and electronic functions on the nanometre scale. Much experimental and theoretical research is necessary not only for exploring the full potential of this approach but also for arriving at relevant nanostructures that improve the performance of present devices or enable the design of novel ones. The future will reveal how much remains vision and how much can be realized. At any rate, the exploration of the nanometre regime brings about powerful new degrees of freedom for engineering ionically active materials.

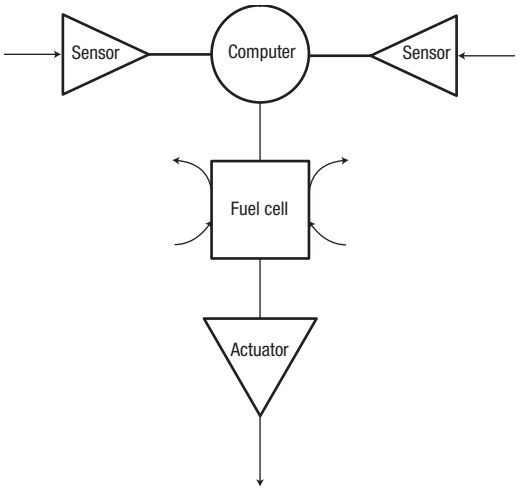

Figure 7 The nano-integration of ionic and electronic 'organs' such as sensors, actuators, computers and fuel cells or batteries results in tiny artificial autonomous systems. Reprinted from ref. 2. Copyright (2004) with permission from John Wiley & Sons Ltd.

doi:10.1038/nmat1513

References

1. Kudo, T. & Fueki, K. *Solid State Ionics* (Kodansha, Tokyo, 1990).
2. Maier, J. *Physical Chemistry of Ionic Materials. Ions and Electrons in Solids* (Wiley, Chichester, 2004).
3. Bruce, P. G. *Solid State Electrochemistry* (Cambridge Univ. Press, London, 1995).
4. Bouwmeester, H. J. M. & Gellings, P. J. *Solid State Electrochemistry* (CRC Press, New York, 1997).
5. Maier, J. Point defect thermodynamics: Macro- vs. nanocrystals. *Electrochemistry* **68,** 395–402 (2000).
6. Maier, J. Aspects of nano-ionics, part I. Thermodynamic aspects and morphology of nano-structured ion conductors. *Solid State Ionics* **154,** 291–301 (2002); Part II. Defect chemistry and ion transport in nanostructured materials. *Solid State Ionics* **157,** 327–334 (2003); Part III. Nano-sized mixed conductors. *Solid State Ionics* **148,** 367–374 (2002).
7. Maier, J. Nano-ionics: Trivial and non-trivial size effects on ion conduction in solids. *Z. Phys. Chem.* **217,** 415–436 (2003).
8. Maier, J. Space charge regions in solid two phase systems and their conduction contribution. III: Defect chemistry and ionic conductivity in thin films. *Solid State Ionics* **23,** 59–67 (1987).
9. Brus, L. E. Electron–electron and electron–hole interactions in small semiconductor crystallites: The size dependence of the lowest excited electronic state. *J. Chem. Phys.* **80,** 4403–4409 (1984).
10. Reed, M. & Kirle, W. P. *Nanostructure Physics and Fabrication* (Academic, New York, 1989).
11. Haug, R. J. & von Klitzing, K. Prospects for research on quantum dots and single-electron transistors. *FED J.* **6,** 4–12 (1995).
12. Ploog, K. in *Semiconductor Interfaces: Formation and Properties* (eds Lay, G. L., Derrien, J. & Boccara, N.) 10–42 (Springer Proceedings in Physics 22, Berlin, 1987).
13. Sze, S. M. *Semiconductor Devices* (Wiley, New York, 1985).
14. Jonker, G. H. Some aspects of semiconducting barium titanate. *Solid State Electronics* **7,** 895–903 (1964).

15. Seiyama, T., Kato, A., Fujiishi, K. & Nagatani, M. A new detector for gaseous components using semiconductive thin films. *Anal. Chem.* **34,** 1502–1503 (1962).
16. Maier, J. Ionic transport in nano-sized systems. *Solid State Ionics* **175,** 7–12 (2004).
17. Maier, J. Ionic conduction in space charge regions. *Prog. Solid State Chem.* **23,** 171–263 (1995).
18. Tuller, H. L. Ionic conduction in nanocrystalline materials. *Solid State Ionics* **131,** 143–157 (2000).
19. Schoonman, J. Nanostructured materials in solid state ionics. *Solid State Ionics* **135–137,** 5–19 (2005).
20. Jamnik, J. & Maier, J. Nanocrystallinity effects in lithium battery materials. (Aspects of nano-ionics. Part IV). *Phys. Chem. Chem. Phys.* **5,** 5215–5220 (2003).
21. Despotuli, A. L. & Nikolaichik, V. I. A step towards nanoionics. *Solid State Ionics* **60,** 275–278 (1993).
22. Chapman, D. L. A contribution to the theory of electrocapillarity. *Phil. Mag. S. 6* **25,** 475–481 (1913).
23. Kliewer, K. L. & Koehler, J. S. Space charge in ionic crystals. I. General approach with application to NaCl. *Phys. Rev. A* **140,** A1226–A1240 (1965).
24. Poeppel, R. B. & Blakely, J. M. Origin of equilibrium space charge potentials in ionic crystals. *Surf. Sci.* **15,** 507–523 (1969).
25. Maier, J. Defect chemistry and conductivity effects in heterogeneous solid electrolytes. *J. Electrochem. Soc.* **134,** 1524–1535 (1987).
26. Jamnik, J., Maier, J. & Pejovnik, S. Interfaces in solid ionic conductors: Equilibrium and small signal picture. *Solid State Ionics* **75,** 51–58 (1995).
27. Puin, W., Rodewald, S., Ramlau, R., Heitjans, P. & Maier, J. Local and overall ionic conductivity in nanocrystalline CaF_2. *Solid State Ionics* **131,** 159–164 (2000).
28. Chiang, Y.-M., Lavik, E., Kosacki, I., Tuller, H. L. & Ying, J. Y. Defect and transport properties of nanocrystalline CeO_{2-x}. *Appl. Phys. Lett.* **69,** 185–187 (1996).
29. Tschöpe, A., Sommer, E. & Birringer, R. Grain size-dependent electrical conductivity of polycrystalline cerium oxide. I. Experiments. *Solid State Ionics* **139,** 255–265 (2001).
30. Vollmann, M. & Waser, R. Grain boundary defect chemistry of acceptor-doped titanates: Space charge layer width. *J. Am. Ceram. Soc.* **77,** 235–243 (1994).
31. Denk, I., Claus, J. & Maier, J. Electrochemical investigations of $SrTiO_3$ boundaries. *J. Electrochem. Soc.* **144,** 3526–3536 (1997).
32. Guo, X., Fleig, J. & Maier, J. Separation of electronic and ionic contributions to the grain boundary conductivity in acceptor-doped $SrTiO_3$. *J. Electrochem. Soc.* **148,** J50–J53 (2001).
33. Leonhardt, M., Jamnik, J. & Maier, J. In situ monitoring and quantitative analysis of oxygen diffusion through Schottky-barriers in $SrTiO_3$ bicrystals. *Electrochem. Solid-State Lett.* **2,** 333–335 (1999).
34. Kim, S. & Maier, J. On the conductivity mechanism of nanocrystalline ceria. *J. Electrochem. Soc.* **149,** J73–J83 (2002).
35. Maier, J. Space charge regions in solid two-phase systems and their conduction contribution. I. Conductance enhancement in the system ionic conductor–'inert' phase and application on $AgCl{\cdot}Al_2O_3$ and $AgCl{\cdot}SiO_2$. *J. Phys. Chem. Solids* **46,** 309–320 (1985).
36. Liang, C. C. Conduction characteristics of lithium iodide aluminium oxide solid electrolytes. *J. Electrochem. Soc.* **120,** 1289–1292 (1973).
37. Chung, R. W. & de Leeuw, S. W. Ionic conduction in LiI-alpha, gamma-alumina: molecular dynamics study. *Solid State Ionics* **175,** 851–855 (2004).
38. Maier, J. & Reichert, B. Ionic transport in heterogeneously and homogeneously doped thallium(I)-chloride. *Ber. Bunsenges. Phys. Chem.* **90,** 666–670 (1986).
39. Lee, J.-S., Adams, S. & Maier, J. Transport and phase transition characteristics in $AgI:Al_2O_3$ composite electrolytes. Evidence for a highly conducting 7-layer AgI polytype. *J. Electrochem. Soc.* **147,** 2407–2418 (2000).
40. Yamada, H., Bhattacharyya, A. J. & Maier, J. Extremely high silver ion conductivity in the composites of silver halide (AgBr, AgI) and mesoporous alumina. *Adv. Funct. Mater.* (in the press).
41. Maekawa, H., Tanaka, R., Sato, T., Fujimaki, Y. & Yamamura, T. Size-dependent ionic conductivity observed for ordered mesoporous alumina-LiI composite. *Solid State Ionics* **175,** 281–285 (2004).
42. Hariharan, K. & Maier, J. Enhancement of the fluoride vacancy conduction in $PbF_2:SiO_2$ and $PbF_2:Al_2O_3$ composites. *J. Electrochem. Soc.* **142,** 3469–3473 (1995).
43. Bhattacharyya, A. J. & Maier, J. Second phase effects on the conductivity of non-aqueous salt solutions: 'soggy sand electrolytes'. *Adv. Mater.* **16,** 811–814 (2004).
44. Croce, F., Appetechi, G. B., Persi, L. & Scrosati, B. Nanocomposite polymer electrolytes for lithium batteries. *Nature* **394,** 456–458 (1998).
45. Wieczorek, W., Florjanczyk, Z. & Stevens, R. Composite polyether based solid electrolytes. *Electrochim. Acta* **40,** 2251–2258 (1995).
46. Kasemägi, H., Aabloo, A., Klintenberg, M. K. & Thomas, J. O. Molecular dynamics simulation of the effect of nanoparticle fillers on ion motion in a polymer host. *Solid State Ionics* **168,** 249–254 (2004).
47. Maier, J. & Lauer, U. Ionic contact equilibria in solids — implications for batteries and sensors. *Ber. Bunsenges. Phys. Chem.* **94,** 973–978 (1990).
48. Maier, J. Space charge regions in solid two phase systems and their conduction contribution. II. Contact equilibrium at the interphase of two ionic conductors and the related conductivity effect. *Ber. Bunsenges. Phys. Chem.* **89,** 355–362 (1985).
49. Shahi, K. & Wagner, J. B. Fast ion transport in silver halide solid solutions and multiphase systems. *Appl. Phys. Lett.* **37,** 757–759 (1980).
50. Sata, N., Eberman, K., Eberl, K. & Maier, J. Mesoscopic fast ion conduction in nanometre-scale planar heterostructures. *Nature* **408,** 946–949 (2000).
51. Jin-Phillipp, N. Y. *et al.* Structures of BaF_2-CaF_2 heterolayers and their influences on ionic conductivity. *J. Chem. Phys.* **120,** 2375–2381 (2004).
52. Petuskey, W. Interfacial effects on Ag:S nonstoichiometry in silver sulfide/alumina composites. *Solid State Ionics* **21,** 117–129 (1986).
53. Beaulieu, L. Y., Larcher, D., Dunlap, R. A. & Dahn, J. R. Reaction of Li with grain-boundary atoms in nanostructured compounds. *J. Electrochem. Soc.* **147,** 3206–3212 (2000).
54. Brankovic, S. R., Wang, J. X. & Adžić, R. R. A. Pt submomolayers on Ru nanoparticles. a novel low Pt loading, high CO tolerance fuel cell electrocatalyst. *Electrochem. Solid-State Lett.* **4,** A217–A220 (2001).
55. Simkovich, G. & Wagner, C. The role of ionic point defects in the catalytic activity of ionic crystals. *J. Catal.* **1,** 521–525 (1962).
56. Maier, J. & Murugaraj, P. The effect of heterogeneous doping on heterogeneous catalysis: Dehydrohalogenation of tertiary butyl chloride. *Solid State Ionics* **40/41,** 1017–1020 (1990).
57. Lipowsky, R. in *Springer Proceedings in Physics* Vol. 50 (eds Falicov, L. M., Mejia-Lira, F. & Morán-López, J. L.) 158–166 (Springer, Berlin, 1990).
58. Hainovsky, N. & Maier, J. Simple phenomenological approach to premelting and sublattice melting in Frenkel disordered ionic crystals. *Phys. Rev. B* **51,** 15789–15797 (1995).
59. Sata, N., Eberman, K., Eberl, K. & Maier, J. Mesoscopic fast ion conduction in nanometre-scale planar heterostructures. *Nature* **408,** 946–949 (2000).
60. Guo, Y.-G., Lee, J.-S. & Maier, J. AgI nanoplates with mesoscopic superionic conductivity at room temperature. *Adv. Mater.* (in the press).
61. Balaya, P., Jamnik, J. & Maier, J. Mesoscopic size effects in nanocrystalline $SrTiO_3$. *Appl. Phys. Lett.* (submitted).
62. Heifets, E., Kotomin, E. A. & Maier, J. Semi-empirical simulations of surface relaxation for perovskite titanates. *Surf. Sci.* **462,** 19–35 (2000).
63. Buffat, P. & Borel, J.-P. Size effect on the melting temperature of gold particles. *Phys. Rev. A* **13,** 2287–2298 (1976).
64. Knauth, P., Schwitzgebel, G., Tschöpe, A. & Villain, S. Emf measurements on nanocrystalline copper-doped ceria. *J. Solid State Chem.* **140,** 295–299 (1998).
65. Schroeder, A. *et al.* Excess free enthalpy of nanocrystalline silver, determined in a solid electrolyte cell. *Solid State Ionics* **173,** 95–101 (2004).
66. Martin, T. P. In *Festkörperprobleme*, *Advances in Solid State Physics* (ed. Grosse, P.) 1–24 (Vieweg, Braunschweig, 1984).
67. Adams, S., Hariharan, K. & Maier, J. Interface effect on the silver ion conductivity during the crystallization of $AgI\text{-}Ag_2O\text{-}V_2O_5$ glasses. *Solid State Ionics* **75,** 193–201 (1995).
68. Maier, J. Composite electrolytes. *Mater. Chem. Phys.* **17,** 485–498 (1987).
69. Trifonova, A. *et al.* Influence of the reductive preparation conditions on the morphology and on the electrochemical performance of Sn/SnSb. *Solid State Ionics* **168,** 51–59 (2004).
70. Beevers, C. A. & Ross, M. A. S. The crystal structure of 'beta alumina' $Na_2O{\cdot}11Al_2O_3$. *Z. Krist.* **97,** 59–66 (1937).
71. Philips, J. C. *Physics of High-T_c Superconductors* (Academic, Boston, 1983).
72. Simon, A. Clusters of valence electron poor metals — structure, bonding and properties. *Angew. Chem. Int. Edn Engl.* **27,** 159–183 (1988).
73. Maier, J. Nanoionics and soft materials science. In *Nanocrystalline Metals and Oxides. Selected Properties and Applications* (eds Knauth, P. & Schoonman, J.) 81–110 (*Electronic Materials: Science & Technology* Vol. 7, Kluwer Academic, Boston, Massachusetts, 2002).
74. Poizot, P., Laruelle, S., Grugeon, S., Dupont, L. & Tarascon, J.-M. Nano-sized transition-metal oxides as negative electrode materials for lithium-ion batteries. *Nature* **407,** 496–499 (2000).
75. Li, H., Richter, G. & Maier, J. Reversible formation and decomposition of LiF clusters using transition metal fluorides as precursors and their application in rechargeable Li batteries. *Adv. Mater.* **15,** 736–739 (2003).
76. Badway, F., Cosandey, F., Pereira, N. & Amatucci, G. G. Carbon metal fluoride nanocomposites. high-capacity reversible metal fluoride conversion materials as rechargeable positive electrodes for Li batteries. *J. Electrochem. Soc.* **150,** A1318–A1327 (2003).
77. Balaya, P., Li, H., Kienle, L. & Maier, J. Fully reversible homogeneous and heterogeneous Li storage in RuO_2 with high capacity. *Adv. Funct. Mater.* **13,** 621–625 (2003).
78. Aurbach, D. Review of selected electrode–solution interactions which determine the performance of Li and Li ion batteries. *J. Power Sources* **89,** 206–218 (2000).
79. Bhattacharyya, A. J., Dollé, M. & Maier, J. Improved Li-battery electrolytes by heterogeneous doping of nonaqueous Li-salt solutions. *Electrochem. Solid-State Lett.* **7,** A432–A434 (2004).
80. Kreuer, K.-D., Paddison, S. J., Spohr, E. & Schuster, M. Transport in proton conductors for fuel-cell applications: Simulations, elementary reactions, and phenomenology. *Chem. Rev.* **104,** 4637–4678 (2004).
81. Schuster, M. F. H. & Meyer, W. H. Anhydrous proton conducting polymer. *Annu. Rev. Mater. Res.* **33,** 232–261 (2003).
82. Zhou, Y. P., Feng, K., Sun, Y. & Zhou, L. A brief review on the study of hydrogen storage in terms of carbon nanotubes. *Progr. Chem.* **15,** 345–350 (2003).

83. Schlapbach, L. & Züttel, A. Hydrogen-storage materials for mobile applications. *Nature* **414,** 353–358 (2001).
84. Ma, R. Synthesis of boron nitride nanofibers and measurement of their hydrogen uptake capacity. *Appl. Phys. Lett.* **81,** 5225–5227 (2002).
85. Jamnik, J., Kamp, B., Merkle, R. & Maier, J. Space charge influenced oxygen incorporation in oxides: in how far does it contribute to the drift of Taguchi sensors? *Solid State Ionics* **150,** 157–166 (2002).
86. Barsan, N. & Weimar, U. Conduction model of metal oxide gas sensors. *J. Electroceramics* **7,** 143–167 (2001).
87. Pan, X. Q., Fu, L. & Dominguez, J. E. Structure-property relationship of nanocrystalline tin dioxide thin films grown on sapphire. *J. Appl. Phys.* **89,** 6056–6061 (2001).
88. Maier, J. Electrical sensing of complex gaseous species by making use of acid-base properties. *Solid State Ionics* **62,** 105–111 (1993).
89. Holzinger, M., Fleig, J., Maier, J. & Sitte, W. Chemical sensors for acid-base-active gases: Applications to C O_2 and NH_3. *Ber. Bunsenges. Phys. Chem.* **99,** 1427–1432 (1995).
90. Grätzel, M. Photoelectrochemical cells. *Nature* **414,** 338–344 (2001).
91. Maier, J. Ionic and mixed conductors for electrochemical devices. *Radiation Effects Defects Solids* **158,** 1–10 (2003).
92. Maier, J. in *Modern Aspects of Electrochemistry* Vol. 38 (eds Conway, B. E., Vayenas, C. G. & White, R. E.) 1–173 (Springer, New York, 2003).
93. Gambardella, P. *et al.* Ferromagnetism in one-dimensional monatomic metal chains. *Nature* **416,** 301–304 (2002).
94. Kreuer, K.-D., Dippel, T., Meyer, W. & Maier, J. in *Solid State Ionics III* (eds Nazri, G.-A., Tarascon, J.-M. & Armand, M.) 273–282 (*Mat. Res. Soc. Symp. Proc.* Vol. 293, Materials Research Society, Pittsburgh, PA, 1993).
95. Eikerling, M., Kornyshev, A. A., Kuznetsov, A. M., Ulstrup, J. & Walbran, S. Mechanisms of proton conductance in polymer electrolyte membranes. *J. Phys. Chem. B* **105,** 3646–3662.
96. Voet, B. & Voet, J. G. *Biochemistry* (Wiley, New York, 1995).
97. Borg, R. J. & Dienes, G. J. *The Physical Chemistry of Solids* (Academic, San Diego, 1992).
98. Chandra, A. & Maier, J. Properties and morphology of highly conducting inorganic solid-liquid composites based on AgCl. *Solid State Ionics* **145,** 153–158 (2002).
99. Maier, J. Point-defect thermodynamics and size effects. *Solid State Ionics* **131,** 13–22 (2000).

Acknowledgements

The author is indebted to the Max Planck Society and acknowledges support in the framework of the ENERCHEM project.

Competing financial interests

The author declares no competing financial interests.